Measurements of production cross sections of ^{10}Be and ^{26}Al by 120 GeV and 392 MeV proton bombardment of ^{89}Y, ^{159}Tb, and ^{nat}Cu targets

S. Sekimoto[1], S. Okumura[1], H. Yashima[1], Y. Matsushi[2], H. Matsuzaki[3], H. Matsumura[4], A. Toyoda[4], K. Oishi[5], N. Matsuda[6], Y. Kasugai[6], Y. Sakamoto[7], H. Nakashima[6], D. Boehnlein[8], R. Coleman[8], G. Lauten[8], A. Leveling[8], N. Mokhov[8], E. Ramberg[8], A. Soha[8], K. Vaziri[8], K. Ninomiya[9], T. Omoto[9], T. Shima[10], N. Takahashi[9], A. Shinohara[9], M. W. Caffee[11, 12], K.C. Welten[13], K. Nishiizumi[13], S. Shibata[14], T. Ohtsuki[1]

[1] Research Reactor Institute, Kyoto University, Kumatori, Osaka, 590-0494, Japan

[2] Disaster Prevention Research Institute, Kyoto University, Uji, Kyoto, 611-0011, Japan

[3] Department of Nuclear Engineering and Management, School of Engineering, University of Tokyo, Bunkyo, Tokyo, 113-0032, Japan

[4] High Energy Accelerator Research Organization, Tsukuba, Ibaraki, 305-0801, Japan

[5] Shimizu Corporation, Ecchujima, Tokyo, 135-8530, Japan

[6] Japan Atomic Energy Agency, Tokai-mura, Naka-gun, Ibaraki, 319-1195, Japan

[7] ATOX Co., Ltd., Kashiwa, Chiba, 277-0861, Japan

[8] Fermi National Accelerator Laboratory, Batavia, IL 60510 , USA

[9] Graduate School of Science, Osaka University, Toyonaka, Osaka, 560-0043, Japan

[10] Research Center for Nuclear Physics, Osaka University, Suita, Osaka, 567-0047, Japan

[11] Department of Physics and Astronomy, Purdue University, West Lafayette, IN 47907, USA

[12] Department of Earth, Atmospheric, and Planetary Sciences, Purdue University, West Lafayette, IN 47907, USA

[13] Space Sciences Laboratory, University of California, Berkeley, CA 94720-7450, USA

[14] RIKEN Nishina Center for Accelerator-Based Science, Wako, Saitama 351-0198, Japan

Abstract

The production cross sections of ^{10}Be and ^{26}Al were measured by accelerator mass spectrometry using ^{89}Y, ^{159}Tb, and ^{nat}Cu targets bombarded by protons with energies E_p of 120 GeV and 392 MeV. The production cross sections obtained for ^{10}Be and ^{26}Al were compared with those previously reported using E_p = 50 MeV–24 GeV and various targets. It was found that the production cross sections of ^{10}Be monotonically increased with increasing target mass number when the proton energy was greater than a few GeV. On the other hand, it was also found that the production cross sections of ^{10}Be decreased as the target mass number increased from that of carbon to those near the mass numbers of nickel and zinc when the proton energy was below approximately 1 GeV. They also increased as the target mass number increased from near those of nickel and zinc to that of bismuth, in the same proton energy range. Similar results were observed in the production cross sections of ^{26}Al, though the absolute values were quite different between ^{10}Be and ^{26}Al. The difference between these production cross sections may depend on the impact parameter (nuclear radius) and/or the target nucleus stiffness.

1. Introduction

When a proton strikes a target nucleus with high energy, the nucleus disintegrates into smaller fragments not only through fission, but also through spallation and/or fragmentation. Normally, observation of a small number of light fragments accompanied with numerous individual nucleons after a reaction indicates spallation. A relatively high-energy process in which nuclides with heavier masses than mass of the above fragments are split from a heavier target nucleus can be called fragmentation. The processes for nuclear disintegration may lead to a variety of final states, characterized by different sizes of fragments. For many years, the study of the processes and their applications has been an attractive field in nuclear physics, nuclear chemistry, and even geo-/cosmochemistry. However, the production cross sections of light and middle-mass nuclides have been scarcely reported owing to difficulty in conductiong measurements. Thus, the mechanism that causes these processes is not yet clear, and the nuclear database is not necessarily sufficient, even with the data accumulated by experimental and theoretical studies conducted so far [1-3]. Therefore, the production cross sections of light and middle-mass nuclides in several targets and at various proton energies are needed, to study experimentally and theoretically the processes in detail, as well as to develop the nuclear database.

Recently, only the production cross sections of light nuclides, such as the long-lived nuclides ^{10}Be and ^{26}Al, have been measured, by using high-energy protons on several targets. These

light nuclide cross-sections have enhanced understanding of the reaction processes and further contributed to the nuclear database, which provides scientifically important information for applications in fields such as geo-/cosmochemistry. For target mass numbers greater than 60, few light nuclide production cross sections have been measured and published so far, and the maximum proton energy used thus far is 12 GeV, for which the production cross sections of ^{10}Be were reported [1]. An extensive program for the measurement of the production cross sections of ^{10}Be and ^{26}Al by using accelerator mass spectrometry (AMS) has also been systematically undertaken in our laboratory in recent years, and some results have been published [4].

In this work, we measured the production cross sections of ^{10}Be and ^{26}Al for ^{89}Y and ^{nat}Cu targets using a proton energy E_p of 120 GeV and those for ^{89}Y, ^{159}Tb, and ^{nat}Cu targets with E_p = 392 MeV. Here, mono-isotope target elements, ^{89}Y and ^{158}Tb, were used to facilitate understanding of the reaction process when ^{10}Be and ^{26}Al are produced. The ^{nat}Cu target was selected to enable systematic investigation of targets with intermediate and large mass numbers. The results were compared to the production cross sections of the light nuclides, ^{10}Be and ^{26}Al, that were produced by targets of various mass numbers when 50 MeV–24 GeV protons were used [1-2, 4-15]. The dependence of the production cross sections of those nuclides on the incident energy and on the target mass number are presented here.

2. Experimental

Proton irradiation at 120 GeV and 392 MeV was performed at the Fermi National Accelerator Laboratory (FNAL) and at the Research Center for Nuclear Physics (RCNP), Osaka University, respectively. The Fermilab Test Beam Facility (FTBF) is a high-energy beam facility devoted to detector research and development for high-energy physics experiments [16]. At FTBF, 120 GeV primary protons can be utilized at certain positions along the approximately 1500-m-long beam line, such as position M01, which was used in this study. The Ring Cyclotron of RCNP is able to supply protons with energies of 80–400 MeV.

To perform irradiation with 120 GeV protons, the target stacks including Y and Cu foils with thicknesses of 447 mg cm^{-2} and 22.4 mg cm^{-2}, respectively, were inserted into the proton beamline at M01 at FNAL. Each target was arranged so that the center of the proton beam would penetrate the center of the target foil. The Y and Cu foils were separately irradiated for 4.417 h and 3.083 h, respectively. The average intensity of the 120 GeV proton beam at M01 at FNAL was measured using a secondary-emission monitor and was estimated to be 1.33×10^9 protons/s for the Y foil and 0.88×10^9 protons/s for the Cu foil. The beam current obtained by this method is consistent with that determined by using the $^{27}Al(p,3pn)^{24}Na$ reaction as a monitor.

On the other hand, the Y and Tb foils with thicknesses of 112 mg cm^{-2} and of 21 mg cm^{-2}, respectively, were each irradiated for 184 s by protons with a mean current of approximately 100 nA at RCNP, while the Cu foils of 89.4 mg cm^{-2} thickness were irradiated for 60 s by protons with a mean current of approximately 1000 nA. The proton beam current was precisely monitored by measuring the electric and magnetic fields in the insulated beam dump using the secondary electron suppressor. Thus, the proton beam current obtained by this method did not require additional corrections and was consistent with the beam current determined by using the $^{27}Al(p,3pn)^{24}Na$ reaction as a monitor. The average beam currents for the Y and Tb foils and for the Cu foils were 6.34×10^{11} protons/s and 6.24×10^{12} protons/s, respectively, for irradiation with 392 MeV protons. In every run, the target foil was sandwiched between guard foils of the same material to monitor the recoil losses and to prevent cross-contamination between the targets.

After irradiation, the target samples were prepared chemically for the AMS measurements. The irradiated Y, Tb, and Cu foils, except for the Cu irradiated at RCNP (E_p = 392 MeV), were dissolved in HNO_3 after adding 200 μg of Be and 500 μg of Al carriers. The Y and Tb were firstly precipitated from their solutions as $Y_2(C_2O_4)_3$ and $Tb_2(C_2O_4)_3$, respectively, by adding oxalic acid. From the Cu sample, the target element was removed by anion exchange. The Be and Al were separated by cation exchange (Dowex 50WX8, 100-200 mesh) using 1 M HCl and 1.5 M HCl, respectively. We confirmed that the use of hydrochloric acid eluents with

such close acidities could successfully separate the Be and Al into two fractions. Each fraction containing beryllium ions (Be^{2+}) or aluminum ions (Al^{3+}) was concentrated and made slightly basic by adding aqueous ammonia to precipitate $Be(OH)_2$ or $Al(OH)_3$, which were then individually rinsed with H_2O. The Be and Al hydroxides were converted into BeO and Al_2O_3, respectively, by heating. The isotopic ratios of $^{10}Be/^{9}Be$ and $^{26}Al/^{27}Al$ in the Y and Tb target foils were determined by AMS at MALT (Micro Analysis Laboratory, Tandem accelerator), University of Tokyo [17] and were normalized by the ^{10}Be and ^{26}Al AMS measurement standards in the KN standard series that was defined and distributed by Nishiizumi [18, 19]. Unfortunately, the Al_2O_3 samples could not be prepared successfully for AMS measurements in the ^{89}Y and ^{159}Tb targets irradiated at RCNP (E_p = 392 MeV). For the Cu foil irradiated at RCNP, the chemical separation scheme was essentially the same as that described by Sekimoto et al. [4]. The AMS measurement of this sample was completed at the PRIME Lab (Purdue Rare Isotope Measurement Laboratory), Purdue University [20].

3. Results and discussion

The measured production cross sections of ^{10}Be from ^{89}Y, ^{159}Tb, and ^{nat}Cu produced with E_p = 120 GeV and 392 MeV are firstly summarized in Table 1. The uncertainties (±1σ) quoted in the production cross sections were obtained by quadratically adding the uncertainties in the AMS and proton fluence measurements (±5%). The production cross sections are also shown

in Fig. 1. The measured production cross sections are compared with the values obtained previously for light nuclides in various target elements produced by protons of different energies (50 MeV–12 GeV) [1-2, 4-14]. As shown in Fig. 1, when the proton energy exceeds a few GeV, the production cross sections of ^{10}Be steadily increase with the target mass number, regardless of E_p. This trend implies that the production cross sections at higher proton energies could depend on nuclear radius of the target, namely the impact parameter. At proton energies below around 1 GeV, the production cross sections of ^{10}Be behave differently and are dependent on E_p. In this region, as the target mass increases from that of carbon to those of nickel and zinc, the production cross sections decrease. On the other hand, the production cross sections increase as the target mass increases from that of yttrium to that of terbium or even to that of bismuth (see Fig. 1). This trend is also supported by the production cross sections obtained for yttrium and bismuth at $E_p \approx$ 300 MeV by Sekimoto et al.[4] and Schumann et al.[5], respectively

Second, the production cross sections of ^{26}Al from ^{89}Y and ^{nat}Cu targets with E_p = 120 GeV and that from ^{nat}Cu with E_p = 392 MeV are summarized in Table 2. Figure 2 presents these data together with other experimental results obtained for production cross sections in the energy range from 300 MeV to 24 GeV. When the proton energy is over a few tens of GeV, even up to 120 GeV, it seems that the production cross sections of ^{26}Al do not always increase with increasing target mass number like they do in the case of ^{10}Be (see Fig. 1). Although

there are few production cross sections of ^{26}Al for targets ranging in mass from that of aluminum to that of zinc, the production cross sections decrease as target mass number increases, as shown in Fig. 2. The decreasing trend of the production cross sections as the target mass increases from that of aluminum to that of zinc is supported by the production cross sections measured by Shibata et al. [1] for aluminum, iron, cobalt, nickel, copper and zinc with E_p = 12 GeV; those measured by Michel et al. [6] for silicon, iron, and nickel with E_p = 600 MeV; those measured by Regnier et al. [7] for silicon and iron with E_p = 24 GeV, and those by Sisterson et al. [8-9] for aluminum and silicon with E_p = 300 MeV. On the other hand, for targets with masses equal to or greater than that of yttrium, the production cross sections of ^{26}Al slightly increase, though the slope is somewhat different from that of ^{10}Be case. This increasing trend from that of yttrium to that of bismuth is supported by the production cross sections measured in this work for yttrium with E_p = 120 GeV, those measured by Shibata et al. [1] for silver and gold with E_p = 12 GeV, those measured by Sisterson et al. [10] for bismuth with $E_p \approx$ 300 MeV and those reported in our previous work [4] for yttrium with $E_p \approx$ 300 MeV.

It is interesting to note that similar trends in the production cross sections of ^{10}Be and ^{26}Al with increasing target masses can be observed when E_p < 1GeV. Here, both of the production cross sections decrease as the target mass number increases to near those of nickel and zinc as a negative slope, while they increase as the target mass increases beyond those of nickel and

zinc as a positive one. The absolute value of the ^{26}Al cross section is one order of magnitude smaller than that of ^{10}Be for heavier target masses in similar incident enegies. It can be qualitatively deduced that the dominant process for the production of ^{10}Be and ^{26}Al by high-energy protons change from spallation to fragmentation as the slope changes from negative to positive as seen in Figs. 1 and 2. Theoretical study is very important for understanding the reaction mechanism, namely production of light nuclides by the bombardment of high energy protons for intermediate and heavy nuclei. However, it should be noted that it is very difficult even now to reproduce realistically the experimental cross sections by the theoretical calculation due to existence of many disintegration channels, even though there are some theoretical approaches, for example, by Schumann et al [5]. Furthermore, it should be noted that the production cross sections of ^{26}Al for Al and Si targets is almost one order of maginitude larger than those of ^{10}Be as see in Fig. 2 (upper left). This phenomenon is inconsistent with the trend in the absolute production cross sections of ^{10}Be and ^{26}Al described above and the studies of nuclear disintegration processes so far [21, 22]. When the combination of projectile (proton) and targets (^{27}Al and ^{nat}Si) is used for reaction, direct and/or semi-direct reactions, namely ^{27}Al(p,pn)^{26}Al and ^{28}Si(p,2pn)^{26}Al, can be dominant in the vicinity of the targets. It may be the reason why a direct reaction leads such large values in the production cross sections of ^{26}Al.

It is well known that nuclei with masses near those of nickel and zinc are stiffer than those of other nuclei. This fact implies that the production cross sections of light nuclides (^{10}Be and ^{26}Al) are affected by the binding energy of the target nucleus, suggesting that the effect of the binding energy, as indicated by the target mass number, still remains for ^{10}Be when $E_p < 1$ GeV and for ^{26}Al even when E_p is greater than a few GeV. The difference in the boundary E_p where the effect remains or not between^{10}Be and ^{26}Al can be due to the emission probability of these light masses from targets, and may depend on the stiffness of each target nucleus.

Finally, it should be noted that production cross sections of light nuclides, including the values obtained in this work, from heavier targets bombarded by several energy of protons are meaningful in connection with several phenomena, such as the propagation of galactic cosmic rays and nucleosynthesis of the light elements in the solar system or in stars [23]. Further studies are in progress that will provide nuclear data for applications in fields such as geo-/cosmochemistry and astrophysics.

Conclusion

The production cross sections of the long-lived nuclides ^{10}Be and ^{26}Al were measured by AMS using the mono-isotopic targets of ^{89}Y and ^{159}Tb as well as ^{nat}Cu bombarded by protons with E_p = 120 GeV and 392 MeV. The obtained production cross sections of ^{10}Be and ^{26}Al were compared with those previously reported using protons with energies between 50 MeV

and 24 GeV and various targets. It was found that the production cross sections of ^{10}Be monotonically increased with increasing target mass number for E_p greater than a few GeV. This trend may imply that the production cross sections of ^{10}Be depend only on the impact parameter between the target and projectile. The production cross sections of ^{10}Be decreased as the target mass number increased from that of carbon to those of nickel and zinc when E_p was below approxymately 1 GeV. However, the cross sections increased as the target mass number increased from near those of nickel and zinc to those of heavier targets, in the same energy range. Similar results were observed in the production cross sections of ^{26}Al, although the absolute values of the ^{26}Al cross sections are quite different from those of the ^{10}Be cross sections. The difference between these cross sections may depend on the target stiffness.

Acknowledgments

The authors express their gratitude to the RCNP for their generous supports in this experiment (RCNP-E298). This work was supported by a grant-in-aid from the Ministry of Education, Science and Culture (KAKENHI 19360432, 21360473, 23656589, 25790081) in Japan, embryonic research project support in Kyoto University Global COE Program "International Center for integrated Research and Advanced Education in Materials Science", Kansai Research Foundation for technology promotion for SS, National Science Foundation (NSF) and National Aeronautics and Space Administration (NASA) for KN and MWC.

Fermilab is a US Department of Energy Laboratory operated under Contract E-AC02-07CH11359 by the Fermi Research Alliance, LLC.

Reference

1. S. Shibata, M. Imamura, H. Nagai, K. Kobayashi, K. Sakamoto, M. Furukawa, and I. Fujiwara, Phys. Rev. C 48 (1993) 2617.

2. R. Michel, M. Gloris, H.-J. Lange, I. Leya, M. Lüpke, U. Herpers, B. Dittrich-Hannen, R. Röse1, Th. Schiekel, D. Filges, P. Dragovitsch, M. Suter, H.-J. Hofmann, W. Wölfli, P.W. Kubik, H. Baur, and R. Wieler, Nucl. Instr. Meth. B, 103 (1995) 183.

3. S. Shibata, M. Imamura, K. Sakamoto, S. Okizaki, S. Shibutani, H. Matsumura, M. Furukawa, I. Fujiwara, H. Nagai and K. Kobayashi, Radiochim. Acta, 80 (1998) 181

4. S. Sekimoto, T. Omoto, H. Joto, T. Utsunomiya, H. Yashima, K. Ninomiya, K.C. Welten, M.W. Caffee, Y. Matsushi, H. Matsuzaki, R. Nakagaki, T. Shima, N. Takahashi, A. Shinohara, H. Matsumura, D. Satoh, Y. Iwamoto, M. Hagiwara, K. Nishiizumi, and S. Shibata, Nucl. Instr. Meth. B, 294 (2013) 475.

5. D. Schumann, J. Neuhausen, R. Michel, V. Alfimov, H.-A. Synal, J.-C. David, and A. Wallner, J. Phys. G: Nucl. Part. Phys. 38 (2011) 065103.

6. R. Michel, B. Dittrich, U. Herpers, F. Peiffer, T. Schiffmann, P. Cloth, P. Dragovitsch, and D. Filges, Analyst (London), Vol.114, p.287 (1989), UK

7. S. Regnier, M. Lagarde, G. N. Simonoff, and Y. Yokoyama, Earth Planet. Sci. Letters, 18 (1973) 9.

8. J.M. Sisterson, K. Kim, A. Beverding, P.A.J. Englert, M. Caffee, A.J.T. Jull, D.J. Donahue, L. McHargue, C. Castaneda, J. Vincent, and R.C. Reedy, Nucl. Instr. Meth. B, 123 (1997) 324.

9. J.M. Sisterson, K. Kim, A. Beverding, P.A.J. Englert, M.W. Caffee, J. Vincent, C. Castaneda, R.C. Reedy, AIP Conf. Proc. 392 (1997) 811.

10. J.M. Sisterson, K. Kim, A. Beverding, P.A.J. Englert, M. w. Caffee, J. Vincent, C. Castaneda, and R.C. Reedy, Conf.on Appl.of Accel.in Res.and Ind. p.811 (1996), USA

11. R. Michel, R. Bodemann, H. Busemann, R. Daunke, M. Gloris, H.-J. Lange, B. Klug, A. Krins, I. Leya, M. Lüpke, S. Neumann, H. Reinhardt, M. Schnatz-Büttgen, U. Herpers, Th. Schiekel, F. Sudbrock, B. Holmqvist, H. Condé, P. Malmborg, M. Suter, B. Dittrich-Hannen, P.-W. Kubik, H.-A. Synal, and D. Filges, Nucl. Instr. Meth. B, 129 (1997) 153.

12. B. Dittrich, U. Herpers, H.J. Hofmann, W. Wölfli, R. Bodemann, M. Lüpke, R. Michel, P. Dragovitsch, and D. Filges, Nucl. Instr. Meth. B, 52 (1990) 588.

13. K.J. Kim, J.M. Sisterson, P.A.J. Englert, M.W. Caffee, R.C. Reedy, J. Vincent, and C. Castaneda, Nucl. Instr. Meth. B, 196 (2002) 239.

14. Th. Schiekel, F. Sudbrock, U. Herpers, M. Gloris, H.-J. Lange, I. Leya, R. Michel, B. Dittrich-Hannen, H.-A. Synal, M. Suter, P.W. Kubik, M. Blann, and D. Filges, Nucl. Instr. Meth. B, 114 (1996) 91.

15. B. Dittrich, U. Herpers, R. Bodemann, M. Lüpke, R. Michel, P. Signer, R. Wieler, H.J. Hofmann, and W. Wölfli, Report from CEC-Countries and CEC to NEANDC, Vol.U, No.312, p.51 (1990), France

16. < http://ppd.fnal.gov/ftbf/ >

17. H. Matsuzaki, C. Nakano, Y. S. Tsuchiya, K. Kato, Y. Maejima, Y. Miyairi, S. Wakasa, and T. Aze, Nucl. Instr. Meth. B 259 (2007) 36.

18. K. Nishiizumi, M. Imamura, M.W. Caffee, J.R. Southon, R.C. Finkel, J. McAninch, Nucl. Instr. Meth. B 258 (2007) 403.

19. K. Nishiizumi, Nucl. Instr. Meth. B 223 (2004) 388.

20. P. Sharma, M. Bourgeois, D. Elmore, D. Granger, M.E. Lipschutz, X. Ma, T. Miller, K. Mueller, F. Rickey, P. Simms, S. Vogt, Nucl. Instr. Meth. B 172 (2000) 112.

21. X. Campi, J. Desbois, E. Lipparini, Phys. Lett. B 142 (1984) 8.

22. G. English, N.T. Porile, E.P. Steinberg, Phys. Rev. C 10 (1974) 2268.

23. F. Yiou, C. Seide, R. Bernas, J. Geophys. Res. 74 (1969) 2447.

Table 1 Production cross sections of ^{10}Be produced by (p,xpyn) reaction

Target	E_p	σ(^{10}Be) (mb)
^{89}Y	392 MeV	0.217 ± 0.019
^{159}Tb	392 MeV	0.418 ± 0.051
^{nat}Cu	392 MeV	0.208 ± 0.011
^{89}Y	120 GeV	8.72 ± 0.54
^{nat}Cu	120 GeV	5.81 ± 0.53

Table 2 Production cross sections of ^{26}Al produced by (p,xpyn) reaction

Target	E_p	σ (^{26}Al) (mb)
^{nat}Cu	392 MeV	0.039 ± 0.004
^{89}Y	120 GeV	0.824 ± 0.052
^{nat}Cu	120 GeV	1.10 ± 0.33

Figure captions

Fig. 1 Target mass number-dependence of production cross sections for ^{10}Be at E_p = 50 MeV–120 GeV.

Solid triangles (E_p = 120 GeV) and diamonds (E_p = 392 MeV) are production cross sections obtained in this work. Inverted open triangles (E_p = 12 GeV), open squares (E_p = 2.6 GeV), open triangles (E_p = 800 MeV), open diamons (E_p = 400 MeV ± 20 MeV), open circles (E_p = 300 MeV ± 20 MeV), the double squares (E_p = 200 MeV ± 10 MeV), and the double circles (E_p = 50 MeV ± 10 MeV) are taken from Ref. [1], Refs. [2, 5], Refs. [2, 8, 12, 15], Refs. [8, 10, 11, 13, 14], Refs. [4, 5, 8, 11, 13, 14], Refs. [8, 10, 11, 13], and Refs. [8, 10, 11, 12], respectively.

Fig. 2 Target mass number-dependence of production cross sections for ^{26}Al at E_p = 300 MeV – 120 GeV.

Solid triangles (E_p = 120 GeV) and circle (E_p = 392 MeV) are production cross sections obtained in this work. Open diamons (E_p = 24 GeV), inverted open triangles (E_p = 12 GeV), double circles (E_p = 600 MeV), and open circles (E_p = 300 MeV ±20 MeV) are taken from Ref. [7], Ref. [1], Ref. [6], and Refs. [4, 8, 9, 10], respectively. Upper left figure is enlargement in the range of target mass number between 26 and 29. Upper right figure is enlargement in the range of target mass number between 53 and 67.

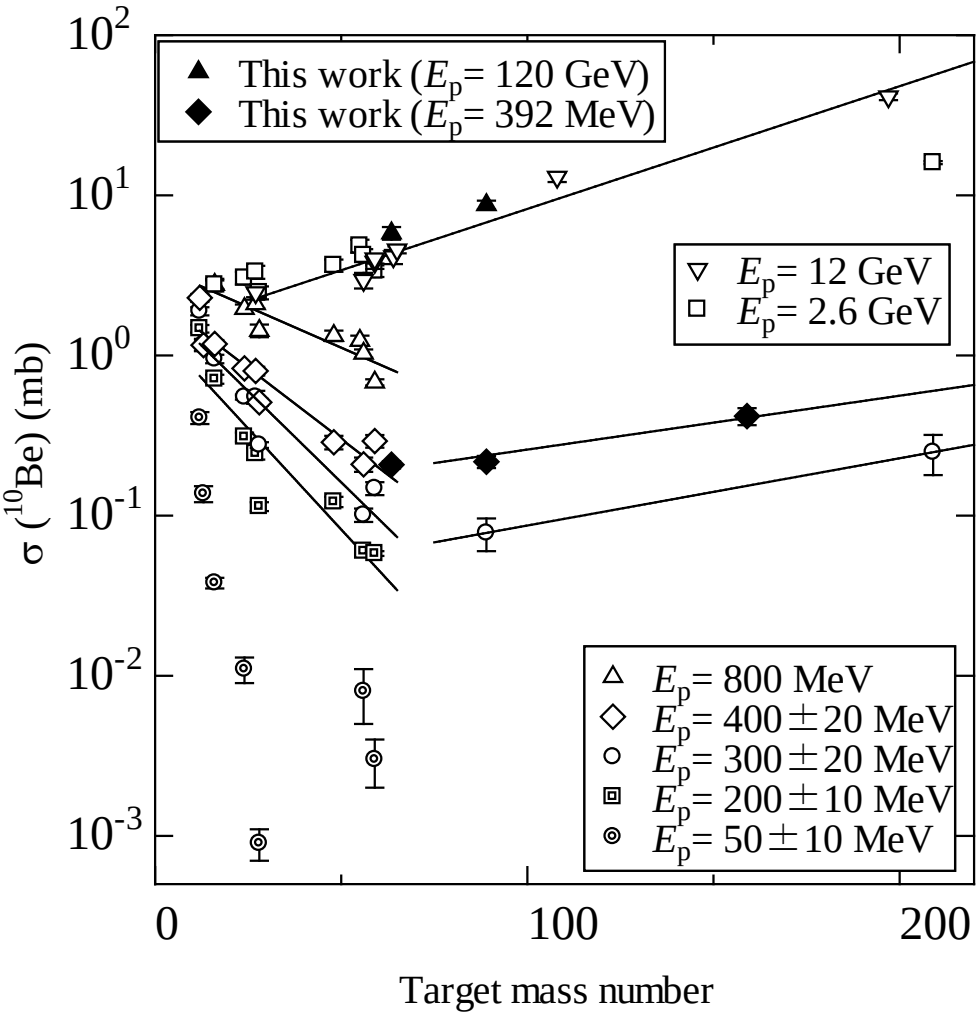
This work (E_p= 120 GeV)
This work (E_p= 392 MeV)
E_p= 12 GeV
E_p= 2.6 GeV
E_p= 800 MeV
E_p= 400±20 MeV
E_p= 300±20 MeV
E_p= 200±10 MeV
E_p= 50±10 MeV
σ (^{10}Be) (mb)
Target mass number
10^2
10^1
10^0
10^{-1}
10^{-2}
10^{-3}
0
100
200

Fig. 1

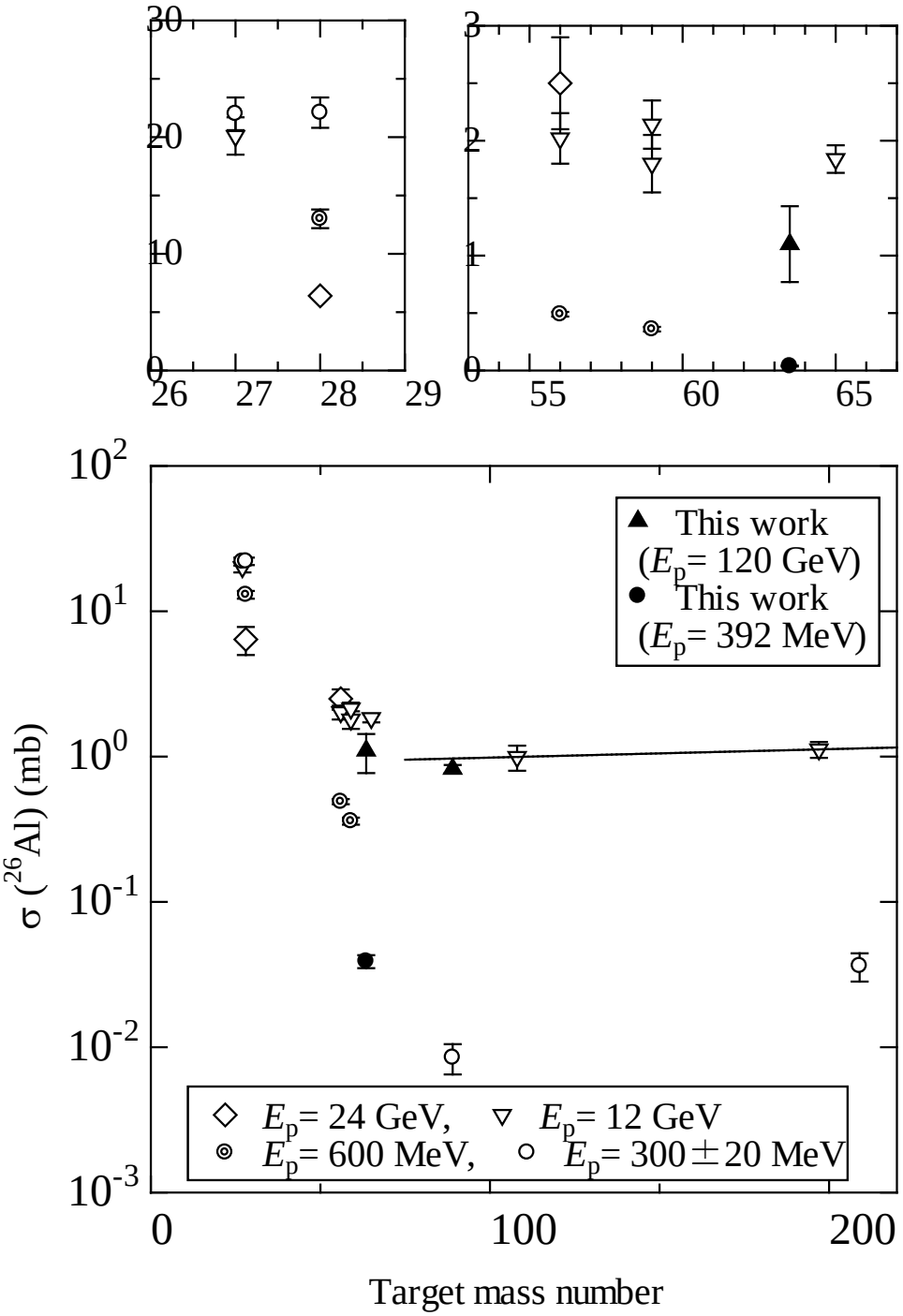
30
20
10
0
26
27
28
29
3
2
1
0
55
60
65
10^2
10^1
10^0
10^{-1}
10^{-2}
10^{-3}
σ (^{26}Al) (mb)
This work
(E_p= 120 GeV)
This work
(E_p= 392 MeV)
E_p= 24 GeV,
E_p= 12 GeV
E_p= 600 MeV,
E_p= 300±20 MeV
0
100
200
Target mass number

Fig. 2